FE/2757-1
Distribution Category UC-90c

HOT LOW BTU PRODUCER GAS DESULFURIZATION IN FIXED BED OF IRON OXIDE-FLY ASH

PROGRESS REPORT NO. 1
12 JULY TO 30 SEPTEMBER 1977

DILIP K. JOSHI

AIR PRODUCTS AND CHEMICALS, INC.
HOUDRY TECHNICAL CENTER
P. O. BOX 427
MARCUS HOOK, PENNSYLVANIA 19061

DATE PUBLISHED - 13 OCTOBER 1977

PREPARED FOR THE DEPARTMENT OF ENERGY
UNDER CONTRACT NO. E(49-18)2757

Blank Page

TABLE OF CONTENTS

PAGE

ABSTRACT 1

I. PROGRESS 2

A. Thermodynamic Evaluation 3

B. Determination of Safe Operating Conditions for Regeneration of Sulfided Sorbents 11

B.1 When Can Actual Temperature Rise in the Bed be Greater than Theoretical Adiabatic Temperature Rise of the Gas 11

B.2 Safe Operating Ranges for the Dimensionless Groups 16

B.3 Safe Operating Ranges for Velocity (V) and Oxygen Concentration (Y_O) 16

B.4 Influence on Process Economics 19

C. Design of the Pilot Plant 19

D. Simulation of Temperature Exotherms and Breakthrough Curves 24

E. Preparation of Guidelines for Economic Evaluation 25

II. FUTURE WORK 25

LIST OF TABLES AND FIGURES

PAGE

Table I Notation 12

Figure 1 Equilibrium Composition for Regeneration of Iron Sulfide by Sulfur Dioxide 5

Figure 2 Equilibrium Composition for Steam Regeneration of Iron Sulfide 6

Figure 3 Equilibrium Conversion for the Reaction H_2S + 1/2 SO_2 = H_2O + 3/2 S 7

Figure 4 Equilibrium Composition for Incomplete Oxidation of Iron Sulfide with Insufficient Air 8

Figure 5 Equilibrium Composition for Air Regeneration of Iron Sulfide (S and SO_2 Production) 9

Figure 6 Equilibrium Composition for Steam-Air Regeneration of Iron Sulfide (S and SO_2 Production) 10

Figure 7 Maximum Bed Temperature Rise Predicted by the Model 15

Figure 8 Determination of Safe Operating Region in Terms of Dimensionless Groups 17

Figure 9 Safe Operating Conditions to Limit Maximum Bed Temperature Below 1500°F 20

Figure 10 Safe Operating Conditions to Limit Maximum Bed Temperature Below 1800°F 21

Figure 11 Horizontal Cross-Section of the Proposed Reactor 22

Figure 12 Schematic Flow Diagram of the Pilot Unit 23

DOE CONTRACT E(49-18)2757

AIR PRODUCTS AND CHEMICALS, INC.
MARCUS HOOK, PENNSYLVANIA 19061

PROGRESS REPORT NO. 1, 12 JULY TO 30 SEPTEMBER 1977

ABSTRACT

This is the first progress report on this APCI project to assist ERDA in the development of their hot producer gas desulfurization process. An iron oxide sorbent will be used in a fixed bed cyclic operation. Specific objectives of this APCI program are: (a) investigation of conditions that yield elemental sulfur as a byproduct during regeneration of sulfided sorbent, (b) preliminary economic analysis, and (c) application of APCI developed mathematical model to MERC data.

During this reporting period, major emphasis was placed in the following areas. Several alternate reaction mechanisms that yield elemental sulfur as a byproduct during regeneration were compared thermodynamically over a wide temperature range. Incomplete oxidation of iron sulfide is the thermodynamically most favored mechanism. Mathematical analysis was done to determine operating conditions that result in bed temperature rises greater than the gas adiabatic temperature rise. The safe operating regions to avoid damage to the sorbent were determined in terms of dimensionless numbers and actual process variables. The test set up for experimental work is designed and necessary equipment is ordered. Using the APCI mathematical model, the entire breakthrough curves and temperature exotherms for two absorption and two regeneration runs were simulated. The predicted breakthrough curves compare very well with the observed breakthrough curves. The predicted temperature exotherms do not agree with the observed temperature exotherms in regeneration, probably due to non-adiabaticity, axial dispersion and side reactions.

DOE CONTRACT E(49-18)2757

AIR PRODUCTS AND CHEMICALS, INC.
MARCUS HOOK, PENNSYLVANIA 19061

PROGRESS REPORT NO. 1, 12 JULY TO 30 SEPTEMBER 1977

This is the second communication concerning progress on the above mentioned contract. It is the first since the contract was formally approved by all parties and, therefore, is numbered as Report No. 1. The previous communication was a letter from L. Friedman to A. I. Berusch, dated 31 August 1977. For completeness, this report covers the progress on the above mentioned contract to date.

This work is undertaken in support of the development of a process for hot stage desulfurization of low Btu producer gas using iron oxide sorbent. Specific objectives of this APCI program are: (a) investigation of conditions that yield elemental sulfur as a byproduct during regeneration of sulfided sorbent, (b) preliminary economic analysis, and (c) application of APCI developed mathematical model to MERC data.

I. PROGRESS

Major emphasis during this period has been in five areas:

A. Thermodynamic evaluation of alternate reaction mechanisms producing elemental sulfur during regeneration.

B. Mathematical analysis to determine operating conditions under which the observed bed temperature rise exceeds the gas adiabatic temperature rise during regeneration of sulfided sorbents.

C. Design of the test set up and ordering necessary equipment.

D. Simulation of temperature exotherms and breakthrough curves observed during absorption and regeneration.

E. Preparation of guidelines for economic evaluation.

Details of this work are described below.

A. Thermodynamic Evaluation

During the experimental work done under ERDA contract E(49-18)2033, it was observed that air-steam regeneration of sulfided iron oxide sorbents produced elemental sulfur as a byproduct. Actual reaction mechanism for this was not known. If the actual reaction mechanism is known, it would help in establishing guidelines to choose operating conditions that would maximize elemental sulfur production.

Three possible reaction mechanisms were identified.

1. Sulfur Dioxide Regeneration

Step I - Sulfur Dioxide Formation

$$FeS + \frac{7}{2} O_2 \rightleftharpoons \frac{1}{2} Fe_2O_3 + SO_2$$

Step II - Elemental Sulfur Formation

$$FeS + \frac{1}{2} SO_2 \rightleftharpoons FeO + \frac{3}{2} S$$

$$FeS + \frac{3}{4} SO_2 \rightleftharpoons \frac{1}{2} Fe_2O_3 + \frac{7}{4} S$$

2. Steam-Sulfur Dioxide Regeneration

Step I - Sulfur Dioxide Formation

$$FeS + \frac{7}{2} O_2 \rightleftharpoons \frac{1}{2} Fe_2O_3 + SO_2$$

Step II - Hydrogen Sulfide Formation

$$FeS + H_2O \rightleftharpoons FeO + H_2S$$

Step III - Claus Reaction

$$H_2S + \frac{1}{2} SO_2 \rightleftharpoons H_2O + \frac{3}{2} S$$

3. Incomplete Oxidation by Air

$$FeS + \frac{1}{2} O_2 \rightleftharpoons FeO + S$$

$$FeS + \frac{3}{4} O_2 \rightleftharpoons \frac{1}{2} Fe_2O_3 + S$$

Sulfur may be formed in several forms, S, S_2, S_3, ..., S_8. In the results discussed below, S is the sum total gm atoms sulfur. That is,

$$S = \sum_i i \cdot Si$$

The thermodynamic analysis was done over a temperature range from 1000°F to 1800°F and simultaneous production of all forms of sulfur was considered. Values of thermodynamic properties were calculated at each temperature and the equilibrium compositions were obtained using a computer program. Given a complex reacting system, this program adjusts the mole fractions of all the molecular species, so as to minimize the free energy of the system. Thermodynamic correlations were based on JANAF tables.

Figures 1 to 6 describe the equilibrium elemental sulfur formation for critical steps in the above reaction mechanisms. In both reaction mechanisms 1 and 2, Step 2 is the critical step.

Figure 1 shows that the reaction between FeS and SO_2, yielding elemental sulfur is negligible up to 1800°F. Hence, sulfur dioxide regeneration does not seem to be the mechanism.

Figure 2 shows that equilibrium conversion for the steam-FeS reaction is very low. Figure 3 shows the equilibrium conversion for Claus reaction where H_2S produced in the steam-FeS reaction reacts with SO_2 produced in FeS-O_2 reaction. The Claus reaction is favored by thermodynamic considerations, but hydrogen sulfide formation (which is necessary for Claus reaction to occur) is not favored. Hence, steam-SO_2 regeneration does not seem to be the mechanism for sulfur production. However, it is possible that any H_2S formed by Step I is immediately reacted in Step II, so that Step I is not at equilibrium.

Figure 4 describes the equilibrium elemental sulfur production for incomplete oxidation of FeS by air. This reaction is thermodynamically favored. Almost all oxygen reacts with iron sulfide to yield elemental sulfur. At low temperature S_8, S_7 and S_6 are the favored forms of sulfur, while at high temperature S_2 is favored. Figure 5 and Figure 6 describe the equilibrium composition when both SO_2 and S formation occur. Equilibrium

FIGURE 1

EQUILIBRIUM COMPOSITION FOR REGENERATION OF IRON SULFIDE BY SULFUR DIOXIDE

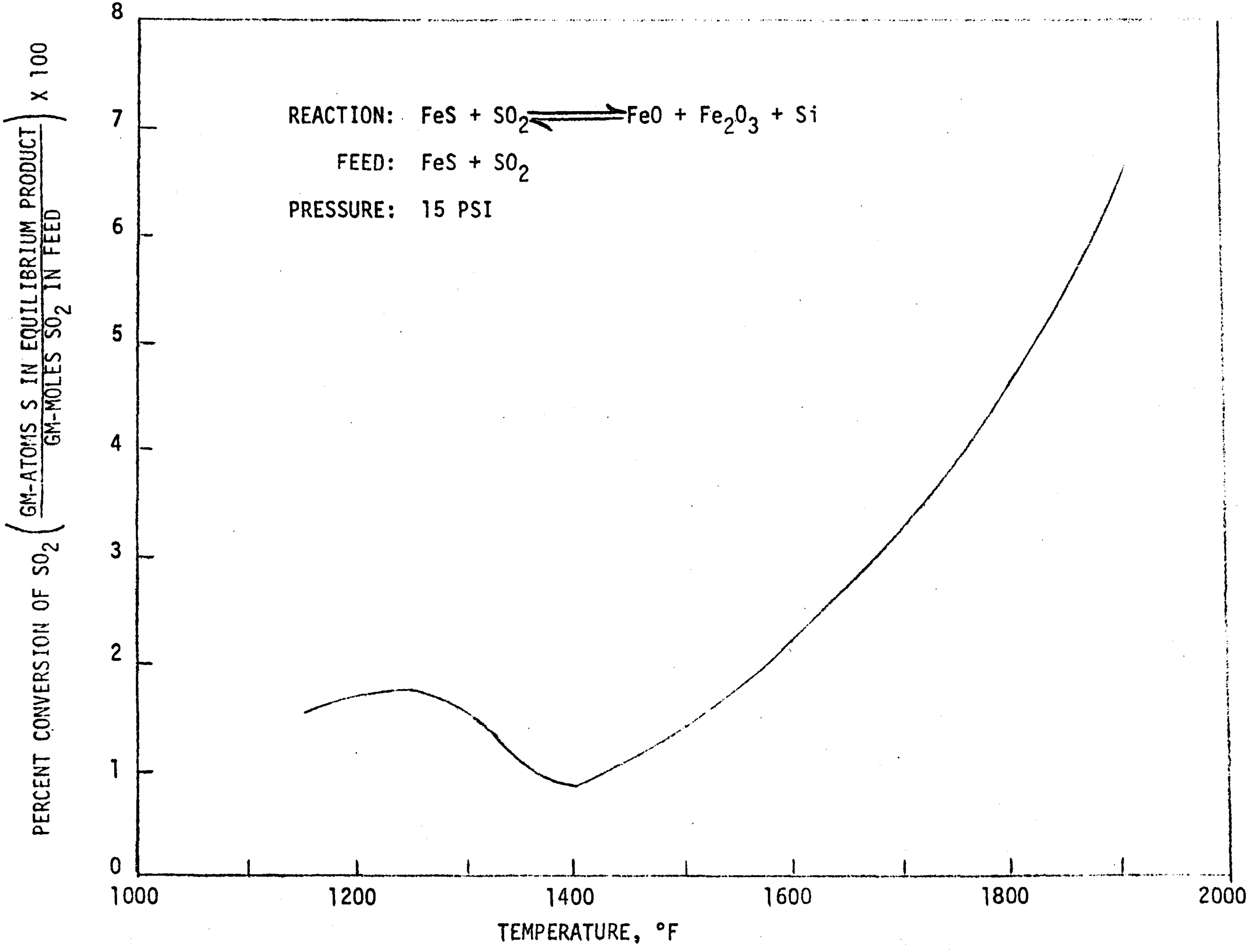

FIGURE 2
EQUILIBRIUM COMPOSITION FOR STEAM REGENERATION OF IRON SULFIDE

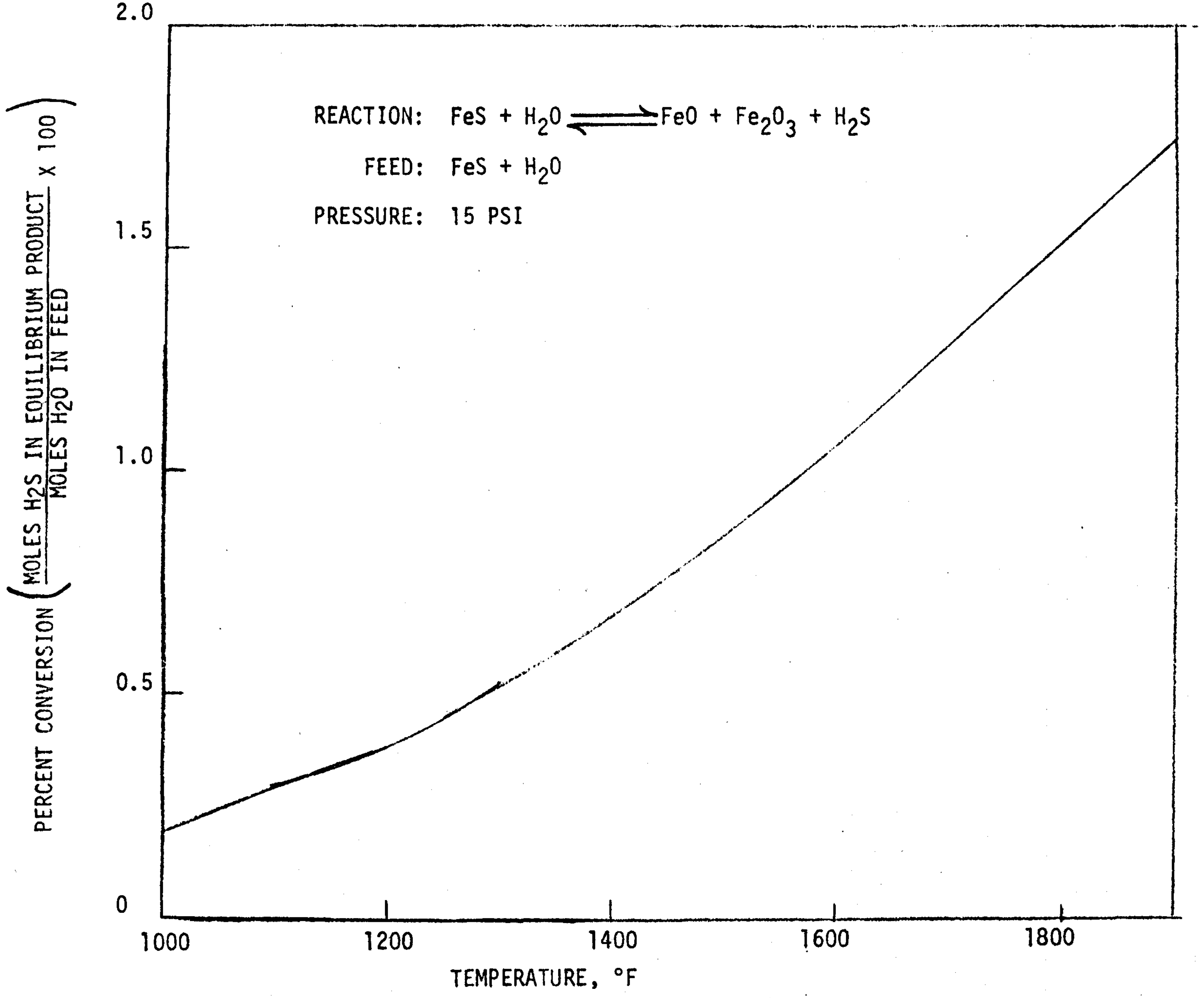

FIGURE 3

EQUILIBRIUM CONVERSION FOR THE REACTION $H_2S + \frac{1}{2} SO_2 = H_2O + \frac{3}{2} S$

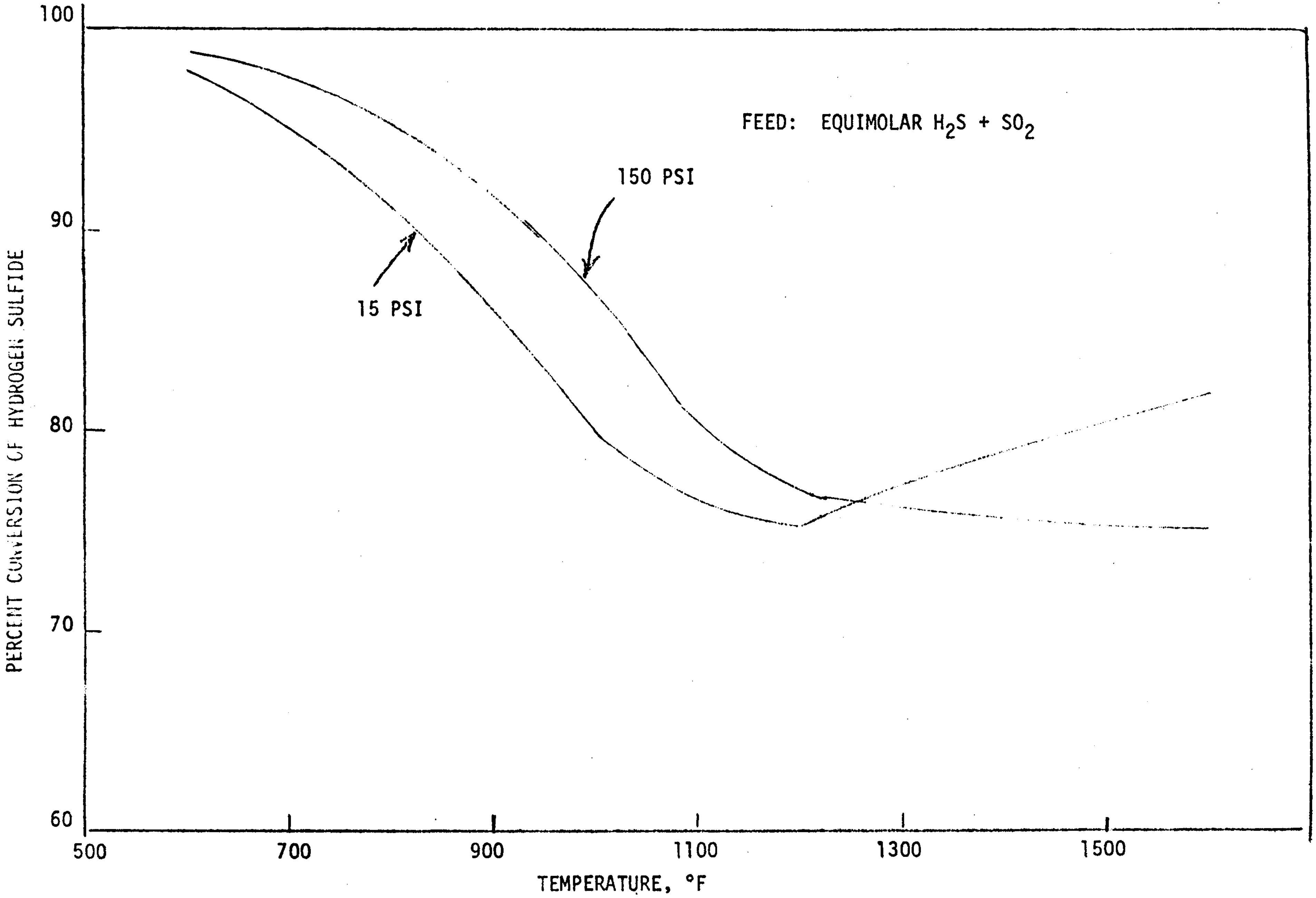

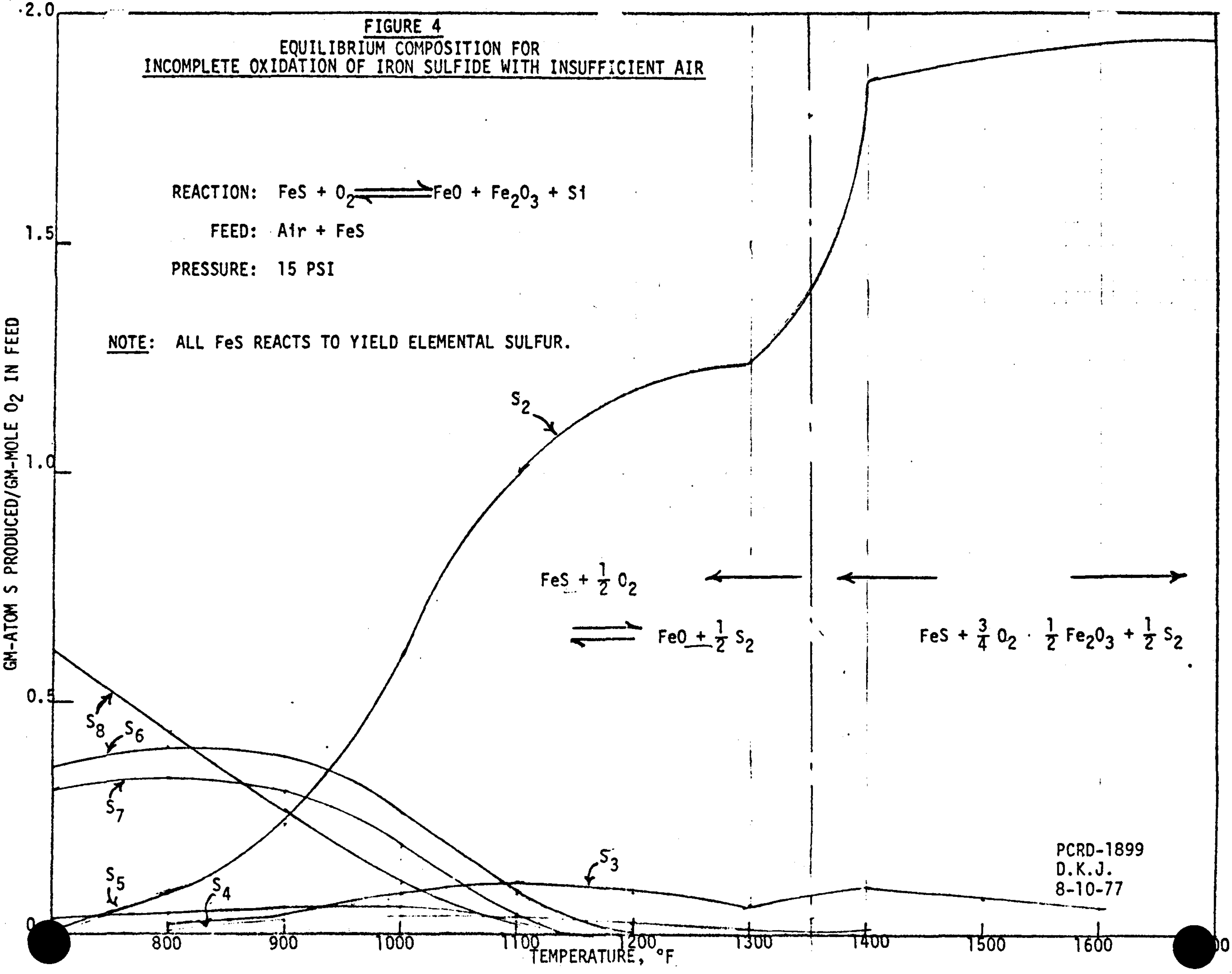

FIGURE 4
EQUILIBRIUM COMPOSITION FOR
INCOMPLETE OXIDATION OF IRON SULFIDE WITH INSUFFICIENT AIR

FIGURE 5

EQUILIBRIUM COMPOSITION FOR AIR REGENERATION OF IRON SULFIDE [S AND SO_2 PRODUCTION]

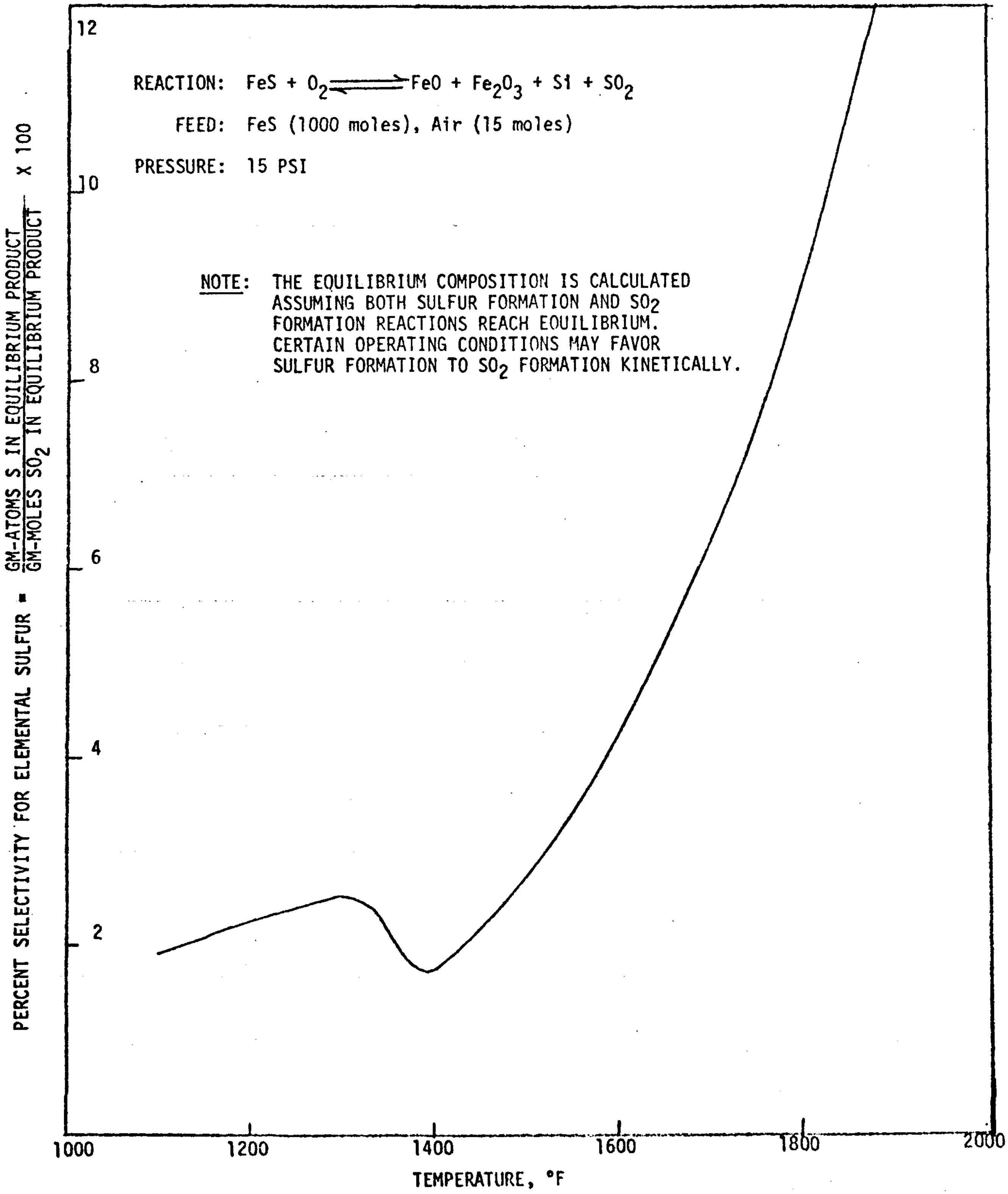

REACTION: $FeS + O_2 \rightleftharpoons FeO + Fe_2O_3 + S1 + SO_2$

FEED: FeS (1000 moles), Air (15 moles)

PRESSURE: 15 PSI

NOTE: THE EQUILIBRIUM COMPOSITION IS CALCULATED ASSUMING BOTH SULFUR FORMATION AND SO_2 FORMATION REACTIONS REACH EQUILIBRIUM. CERTAIN OPERATING CONDITIONS MAY FAVOR SULFUR FORMATION TO SO_2 FORMATION KINETICALLY.

FIGURE 6
EQUILIBRIUM COMPOSITION FOR STEAM-AIR REGENERATION OF IRON SULFIDE
[S AND SO_2 PRODUCTION]

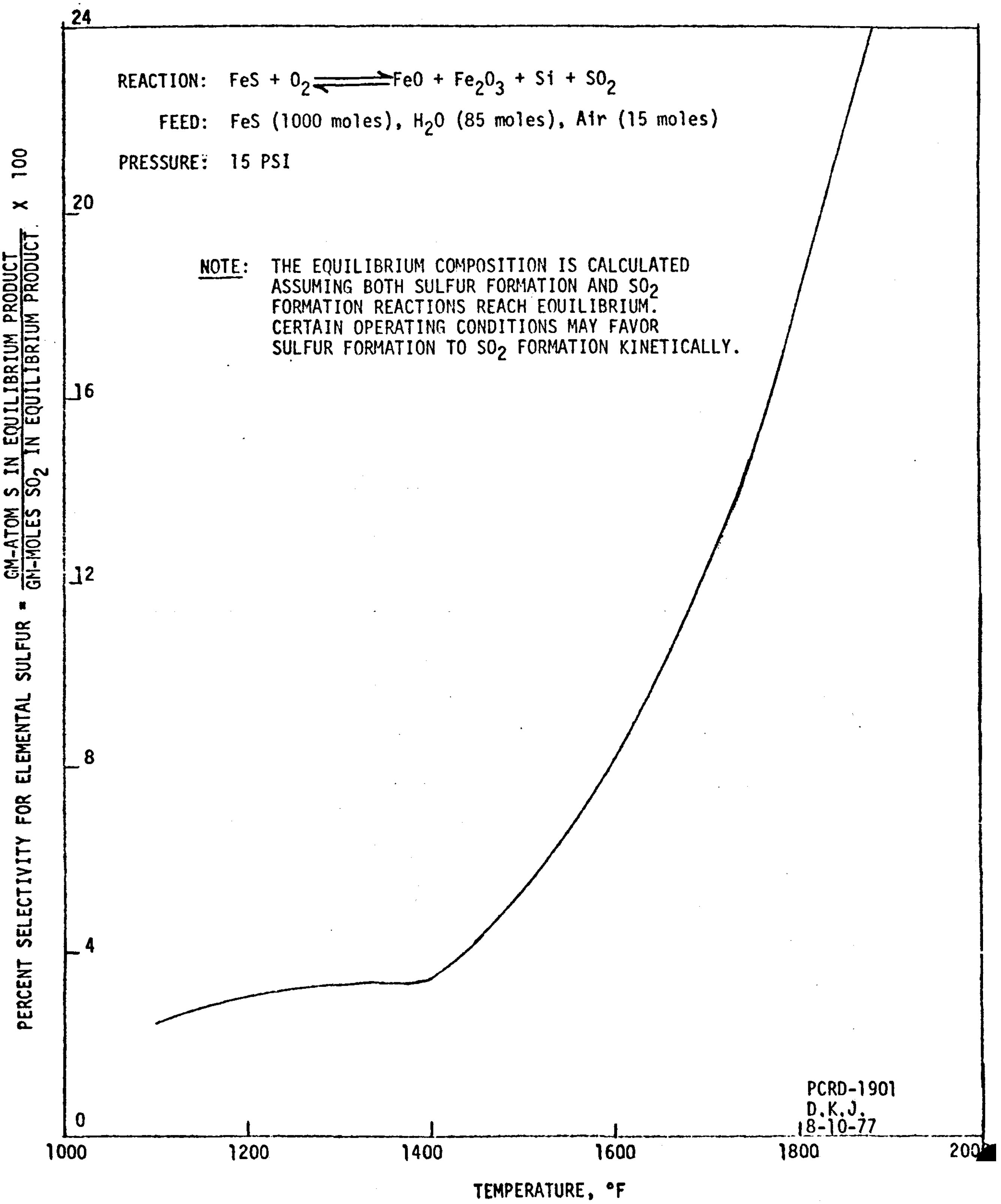

REACTION: $FeS + O_2 \rightleftharpoons FeO + Fe_2O_3 + Si + SO_2$

FEED: FeS (1000 moles), H_2O (85 moles), Air (15 moles)

PRESSURE: 15 PSI

NOTE: THE EQUILIBRIUM COMPOSITION IS CALCULATED ASSUMING BOTH SULFUR FORMATION AND SO_2 FORMATION REACTIONS REACH EQUILIBRIUM. CERTAIN OPERATING CONDITIONS MAY FAVOR SULFUR FORMATION TO SO_2 FORMATION KINETICALLY.

PCRD-1901
D.K.J.
8-10-77

compositions that result in minimum free energy for the entire system yield significant quantities of elemental sulfur. Figure 6 describes the equilibrium for feed composition used in previous experimental work. Significantly higher sulfur formation, probably due to lower partial pressure of oxygen, is observed.

Insufficient oxidation of iron sulfide to produce elemental S is likely to be favored at low oxygen concentrations.

B. Determination of Safe Operating Conditions for Regeneration of Sulfided Sorbents

Regeneration of sulfided iron oxide sorbent is a highly exothermic reaction (heat of reaction 78 kcal/g mole oxygen). Morgantown Energy Research Center has observed bed temperature rises greater than the theoretical adiabatic gas temperature rise under some conditions. It is necessary to limit the maximum temperature that the sorbent "sees" to avoid damage due to sintering which is believed to occur for present absorbents above 1500^{o}F. This report describes how the actual bed temperature rise can be greater than the gas adiabatic temperature rise and how the safe operating region can be determined in terms of dimensionless groups and actual process variables once the maximum allowable temperature rise is chosen. Only the sorbent average temperature is considered and it is possible that particle interior temperatures might exceed those given in this report.

B.1 When Can Actual Temperature Rise in the Bed be Greater than Theoretical Adiabatic Temperature Rise of the Gas?

If we assume that at the beginning of regeneration, iron sulfide concentration throughout the bed is uniform, the analytical treatment described by John Butt (Advances in Chemistry Series 109, ACS (1972) 434-443) may be followed.

Differential equations describing regeneration of sulfided sorbent are given below.

Gas Phase Mass Balance: $$-V \frac{\partial F}{\partial \ell} = (1 - \varepsilon)\, k\, F_W \qquad (1)$$

Overall Mass Balance: $$V_C \frac{\partial F}{\partial \ell} = \frac{\partial W}{\partial t} \qquad (2)$$

Energy Balance: $$V_T \frac{\partial T}{\partial \ell} + (1 + \alpha) \frac{\partial T}{\partial t} = \alpha\, (1 - \varepsilon)\, T_{ab} K\, F_W \qquad (3)$$

Explanation of the symbols used is given in Table I.

TABLE I

NOTATION

DIMENSIONLESS NUMBERS

α	HEAT CAPACITY RATIO	$\frac{C_p C_o}{(1 - \varepsilon) \rho_s C_s}$
$N_{Ab}{}^K$	SORPTION NUMBER	$\frac{V}{\ell k \ (1 - \varepsilon\varepsilon) \ M_B}$
N_{Cp}	HEAT BALANCE NUMBER	$\frac{Y_o C_o \ (1 + \alpha)}{(1 - \varepsilon) \ M_B \ \alpha}$
τ	DIMENSIONLESS TIME	$\frac{V_c t}{\ell}$

OTHER NUMBERS

F	FRACTIONAL BULK GAS O_2 CONCENTRATION
k	PSEUDO FIRST ORDER RATE CONSTANT (hr.$^{-1}$)
M_B	BED OXYGEN CAPACITY (lb. moles/ft.^{3} solid)
ΔT_{Ab}	GAS ADIABATIC TEMPERATURE RISE (^{o}F)
V	SUPERFICIAL GAS VELOCITY AT STP (ft./hr.)
V_c	OXYGEN VELOCITY $\left(\frac{V \ Y_o C_o}{(1 - \varepsilon) \ M_B} \quad \frac{\text{ft.}}{\text{hr.}} \right)$
V_T	BED THERMAL VELOCITY (V α ft./hr.)

TABLE I

NOTATION

- CONTINUED -

OTHER NUMBERS - CONTINUED

w	NORMALIZED BED IRON SULFIDE CONTENT
C_p	SPECIFIC HEAT OF GAS (Btu/lb. moles ^oF)
C_o	MOLAR DENSITY OF GAS (lb. moles/ft.^{3})
ρ	DENSITY OF SOLID

Analytical solution for dimensionless temperature rise is:

$$\theta = \frac{\Delta T}{\Delta T_{Ab}} = \frac{1}{2(1 - N_{Cp})} \left[\tanh\left(\frac{x - \tau}{2N_{Ab}{}^{K}} \right) - \tanh\left(\frac{N_{Cp}\, x - \tau}{2N_{Ab}{}^{K}} \right) \right] \quad (4)$$

This equation may be differentiated for a given bed depth to obtain the value of τ at which the temperature is maximum. Substituting this value of τ, the maximum temperature rise at a given depth during any time in regeneration is given by

$$\frac{\Delta T_{max}}{\Delta T_{Ab}} = \frac{1}{(1 - N_{Cp})} \tanh\left(\frac{x\,(1 - N_{Cp})}{4N_{Ab}{}^{K}} \right) \quad (5)$$

Since hyperbolic tangent has a greater value as the argument increases, the maximum temperature rise will be observed at a depth of $x = 1$, hence, the predicted maximum temperature rise in the bed becomes

$$\frac{\Delta T_{max}}{\Delta T_{Ab}} = \frac{1}{(1 - N_{Cp})} \tanh\left(\frac{(1 - N_{Cp})}{4N_{Ab}{}^{K}} \right) \quad (6)$$

Figure 7 is a plot of the solution of Equation (6) at different kinetic absorption numbers and heat capacity numbers. It can be seen that the maximum bed temperature rise is likely to be greater than the gas adiabatic temperature rise for smaller kinetic absorption number for oxygen. This is not surprising as lower absorption number signifies higher rate of reaction.

FIGURE 7

MAXIMUM BED TEMPERATURE RISE PREDICTED BY THE MODEL

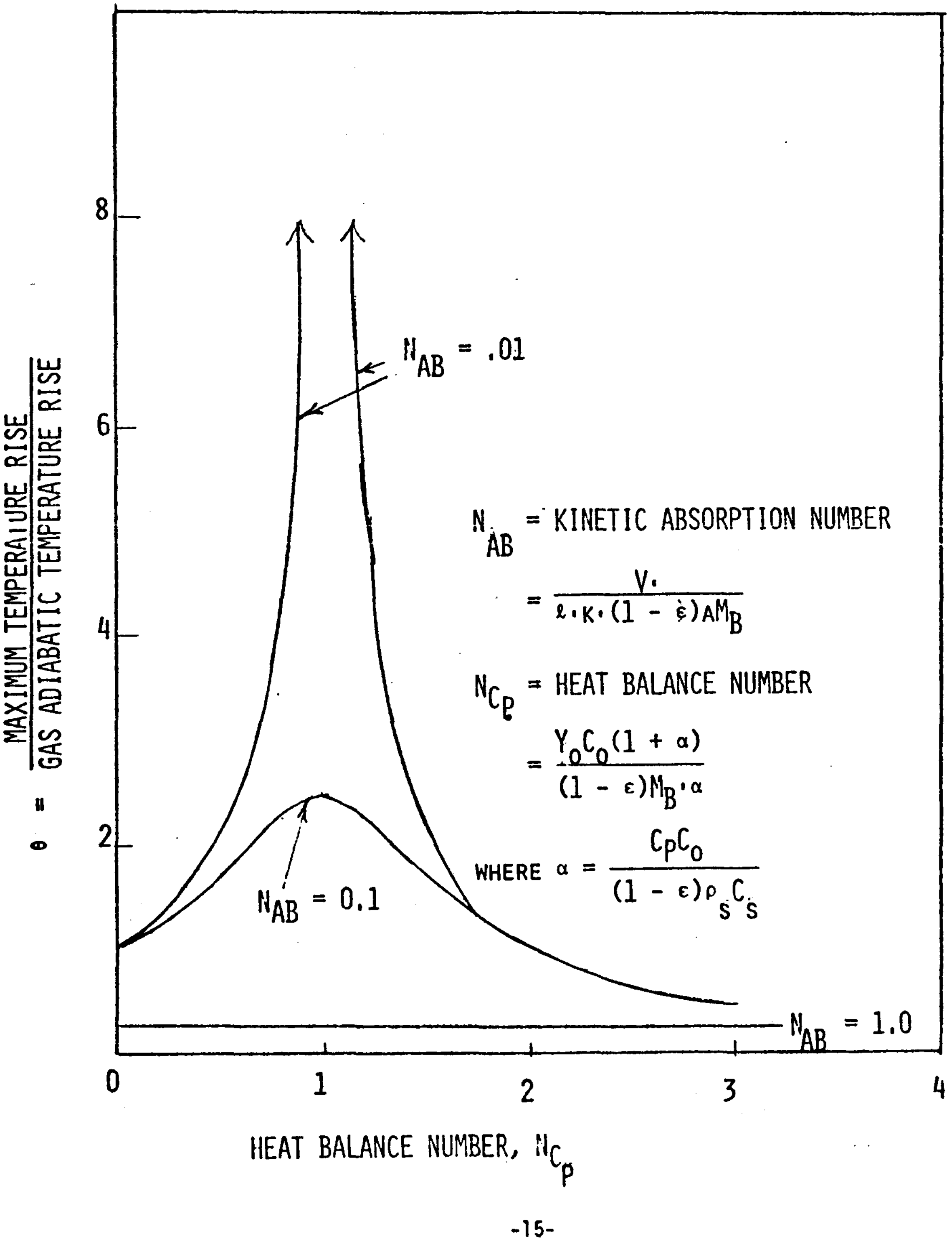

B.2 Safe Operating Ranges for the Dimensionless Groups

For the feed composition used in the regeneration core experimental program, the gas adiabatic temperature rise was 500°F. An inlet temperature of 1000°F and two levels of maximum allowable temperature (1500°F and 1800°F) were chosen. At each maximum allowable temperature, the limiting values of kinetic absorption number for oxygen were calculated for several values of the heat balance number. The resulting plot is a semi-circle (Figure 8). Points lying in the semi-circle result in temperature rises greater than the maximum allowable. At a higher maximum allowable temperature rise, the semi-circle is smaller, illustrating greater operating flexibility. In these calculations, it is assumed that gas adiabatic temperature rise does not change with changes in the heat balance number. This assumption is valid as long as the heat balance number is changed while keeping the oxygen concentration in the feed the same.

B.3 Safe Operating Ranges for Velocity (V) and Oxygen Concentration (Y_o)

An examination of the definitions shows that the gas adiabatic temperature rise is proportional to the oxygen concentration in feed, the absorption number is proportional to velocity and the heat balance number is proportional to oxygen concentration. The proportionality constants were determined in the following manner:

$$N_{Ab}{}^{K} = \frac{V}{I \cdot k \cdot (1 - \varepsilon) M_B} \qquad (7)$$

(Explanation of all the symbols used in this report is given in Table I.)

From experimental data collected in regeneration core experimental program, λ = .883 ft., sulfur wt.% in sorbent = 21.9, and M_B = 1.71 lb. moles oxygen/ft.^{3} solid. In a typical experiment (Run No. 1815SG) N_{Ab} was .1518 at inlet conditions as calculated from the slope of in (F/1-F) vs. τ. This gives $k\ (1 - \varepsilon)\alpha$ to be 5304. Substituting these values

$$N_{Ab}{}^{K} = .0001249\ V \qquad (8)$$

where V is superficial velocity at STP in. ft./hr.

$$N_{Cp} = \frac{Y_o,\ C_o\ (1 + \alpha)}{(1 - \varepsilon)\ M_B \alpha} \qquad (9)$$

FIGURE 8

DETERMINATION OF SAFE OPERATING REGION IN TERMS OF DIMENSIONLESS GROUPS

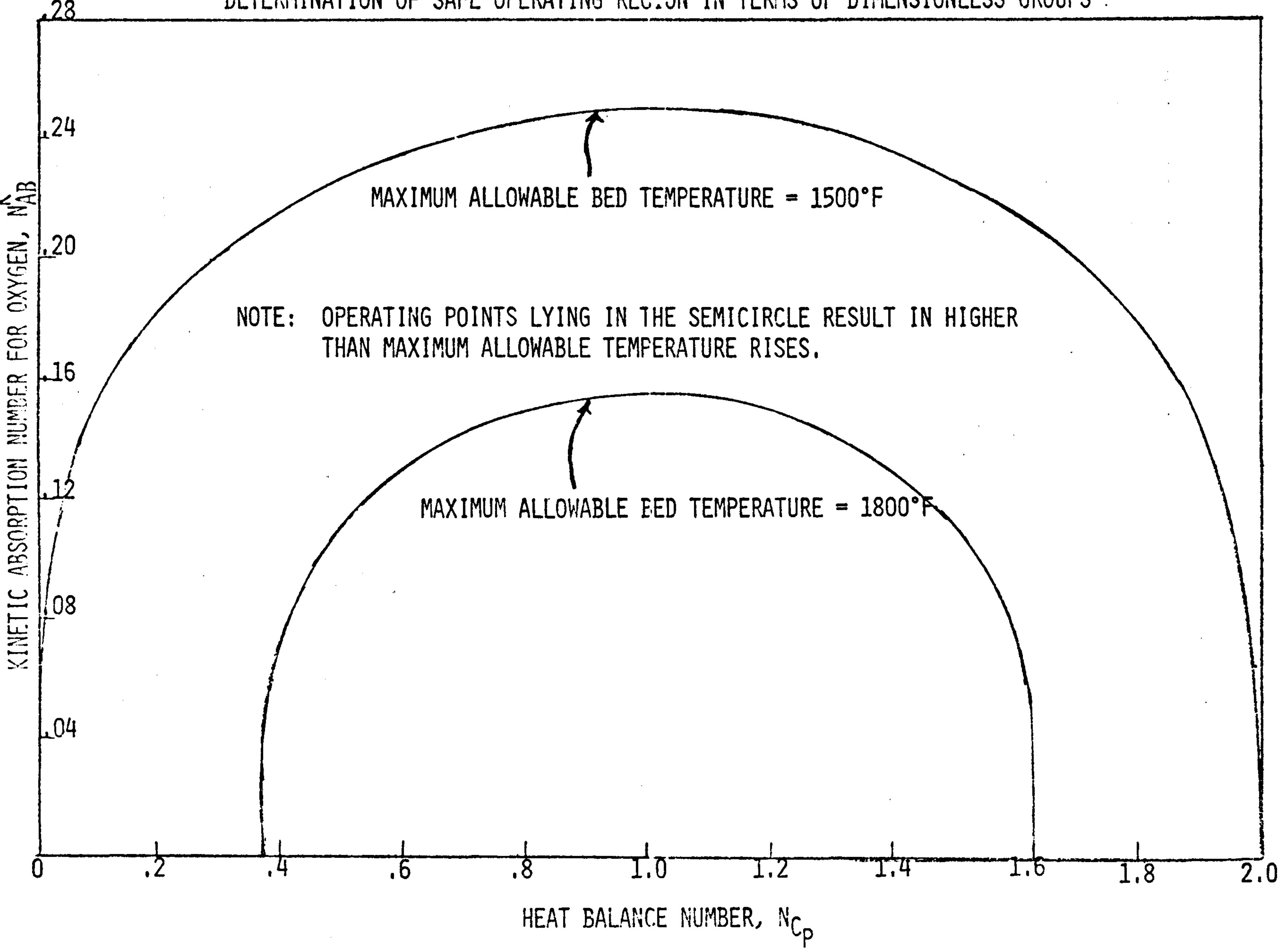

At 30 psig and 1000°F, C_o is .00285 lb. moles/ft.^{3} α = .00197. Then,

$$N_{Cp} = 1.4092\ Y_o \tag{10}$$

where Y_o is the mole fraction of oxygen.

Similarly,

$$\Delta T_{Ab} = 17241\ Y_o \tag{11}$$

Substituting these in Equation (6),

$$\Delta T_{max} = 17241\ Y_o \left[\frac{1}{(1 - 1.4092\ Y_o)}\ \tanh\left(\frac{1 - 1.4092\ Y_o}{4 \times .0001249\ V}\right)\right] \tag{12}$$

This equation is solved for inlet temperature of 1000°F and maximum bed temperatures of 1500 and 1800°F. The proportionality constants depend in wt.% sulfur in the sorbent in the following manner,

$$\frac{N_{Cp_1}}{N_{Cp_2}} = \frac{M_{B_2}}{M_{B_1}} = \frac{S_2}{S_1}$$

where S is wt.% sulfur in sorbent

$$\frac{N_{Ab_1}}{N_{Ab_2}} = \frac{M_{B_2}}{M_{B_1}} = \frac{S_2}{S_1}$$

Wt.% Sulfur	N_{Ab}	N_{Cp}
36.8	.0000743 V	.8386 Y_o
10	.000274 V	3.0861 Y_o
5	.000547 V	6.1773 Y_o

Equation (6) is solved for four different wt.% sulfur in sorbent and two different allowable temperature rises. Solutions are plotted in Figure 9 and Figure 10. Operating points lying to the left of the curve result in bed temperatures lower than the maximum allowable. As expected, a higher allowable maximum temperature allows use of higher oxygen concentration and results in greater operating flexibility. Also, for a given maximum allowable bed temperature it is possible to use high oxygen concentration if the sulfur content of the sulfided sorbent is lower.

B.4 Influence on Process Economics

This observation is significant. For economically attractive processing of the SO_2 containing regeneration effluents, SO_2 concentration should be sufficiently high (= 15%). In regeneration schemes proposed earlier, a recycle stream was included to maintain high SO_2 concentration without exceeding the maximum bed temperature. Figures 9 and 10 show that it is possible to have air with no recycle as the regeneration mode to obtain effluents with high SO_2 concentration, without exceeding allowable temperature rise, if sulfur wt.% in the sorbent is sufficiently low. This would make regeneration more economical, however, lower wt.% S in sulfided sorbent also means lower onstream time in the absorption. Lower wt.% S in sulfided sorbent is likely to make absorption uneconomical due to large reactor and short onstream time.

C. Design of the Pilot Plant

The proposed pilot plant consists of two 3½" diameter and 18" long reactor blocks made of Inconel 601, each consisting of two 3/4" diameter reactors and preheaters. One of the blocks will be used for sulfiding sorbent and the other for regeneration. Temperatures will be measured in the block instead of bed. Flow controllers will be used to maintain constant flows in the reactors. Gas flows will be introduced through a manifold containing rotameter assembly and water will be introduced by syringe pumps. Figure 11 is a cross-section of the proposed reactor block and Figure 12 is a schematic diagram of the proposed pilot plant. Piping will be of Inconel 601 or Inconel 800.

The necessary pieces of equipment have been sized. We plan to use many items from the old ERDA unit. We have received new syringe pumps, some rotameters and flow controllers. The reactor blocks are expected in the middle of October, after which they will be machined to make reactors.

FIGURE 9

SAFE OPERATING CONDITIONS TO LIMIT MAXIMUM BED TEMPERATURE BELOW 1500°F

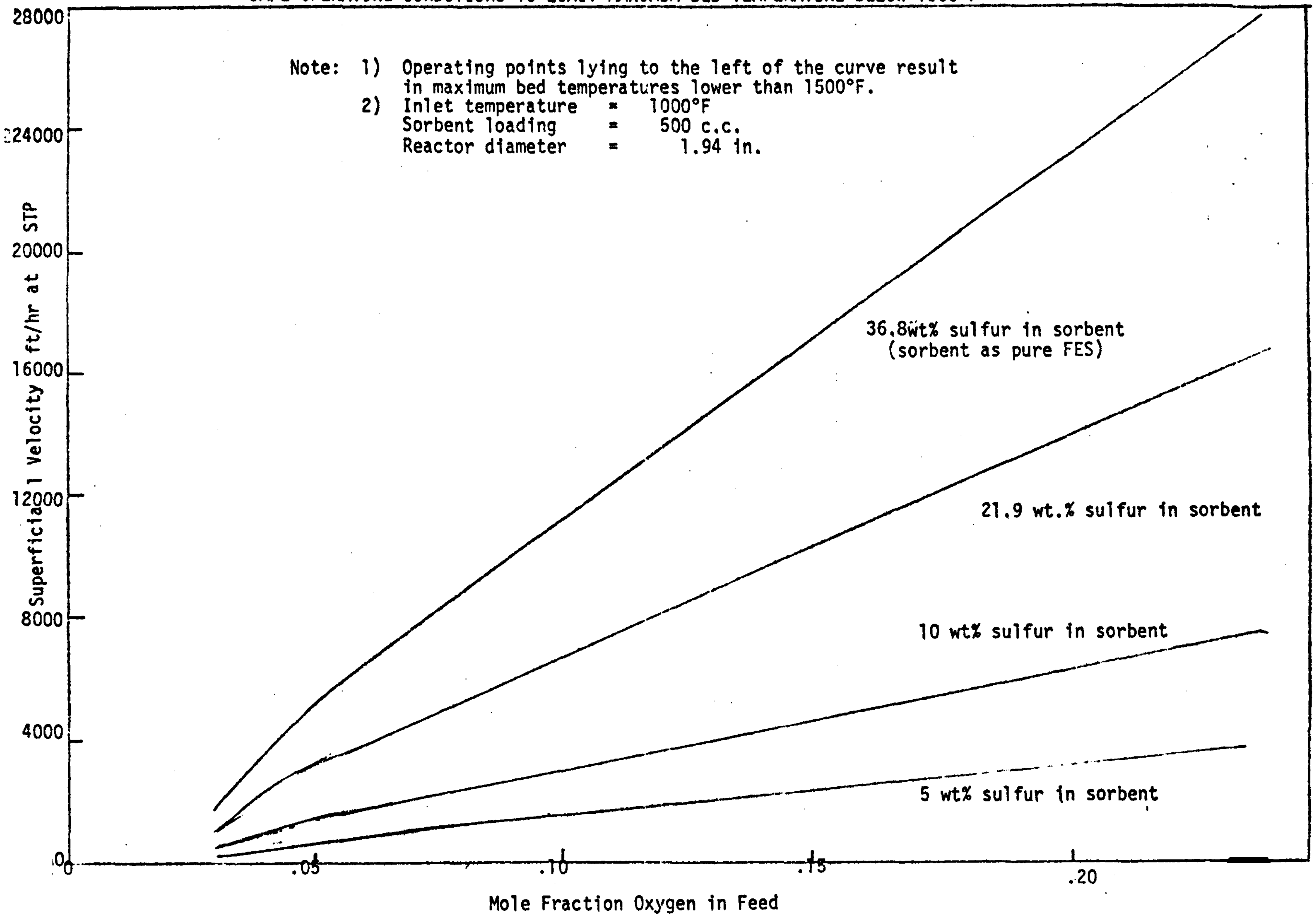

Note: 1) Operating points lying to the left of the curve result in maximum bed temperatures lower than 1500°F.
2) Inlet temperature = 1000°F
Sorbent loading = 500 c.c.
Reactor diameter = 1.94 in.

FIGURE 10

SAFE OPERATING CONDITIONS TO LIMIT MAXIMUM BED TEMPERATURE BELOW 1800°F

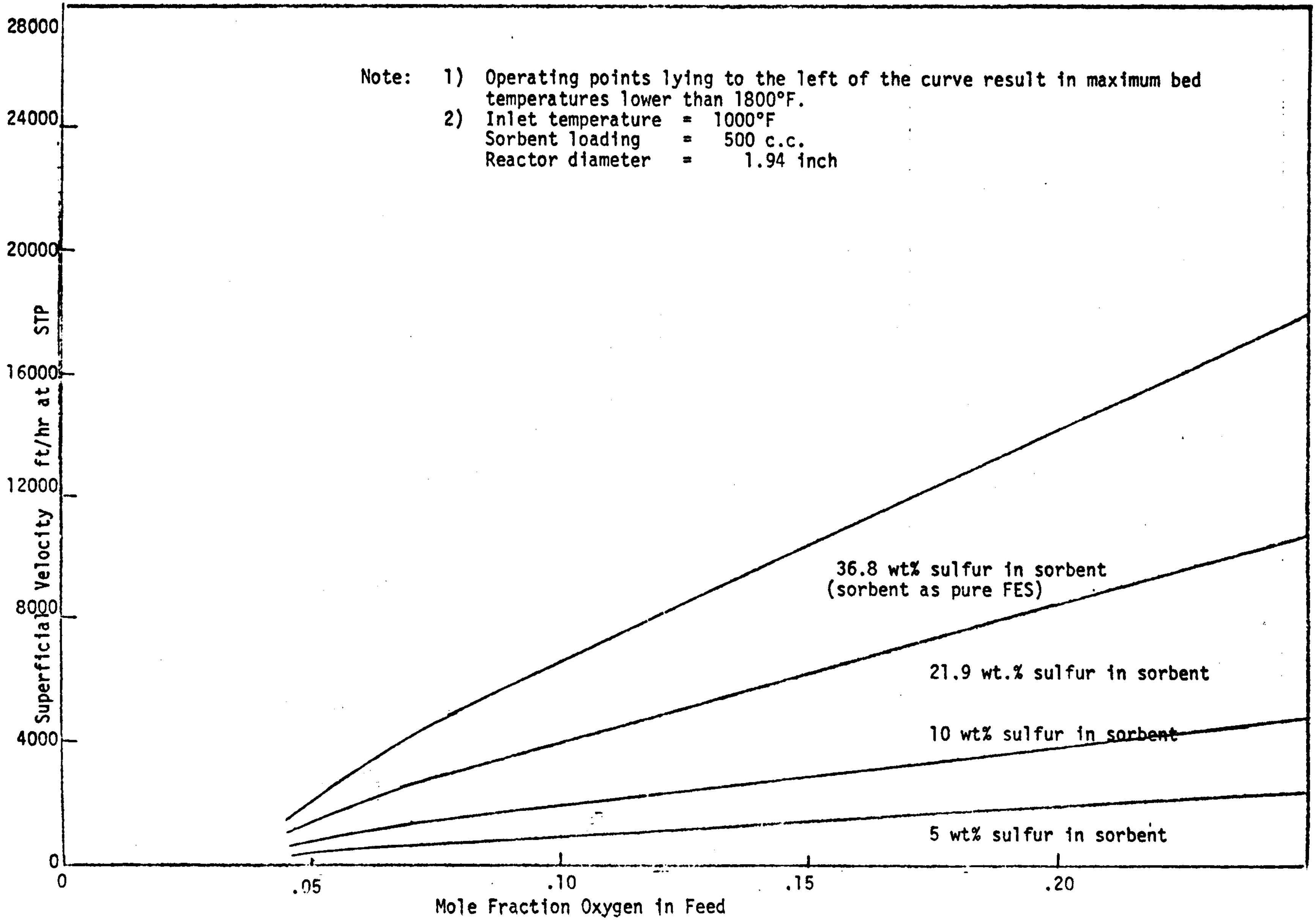
Note: 1) Operating points lying to the left of the curve result in maximum bed temperatures lower than 1800°F.
2) Inlet temperature = 1000°F
Sorbent loading = 500 c.c.
Reactor diameter = 1.94 inch

FIGURE 11

HORIZONTAL CROSS-SECTION OF THE PROPOSED REACTOR

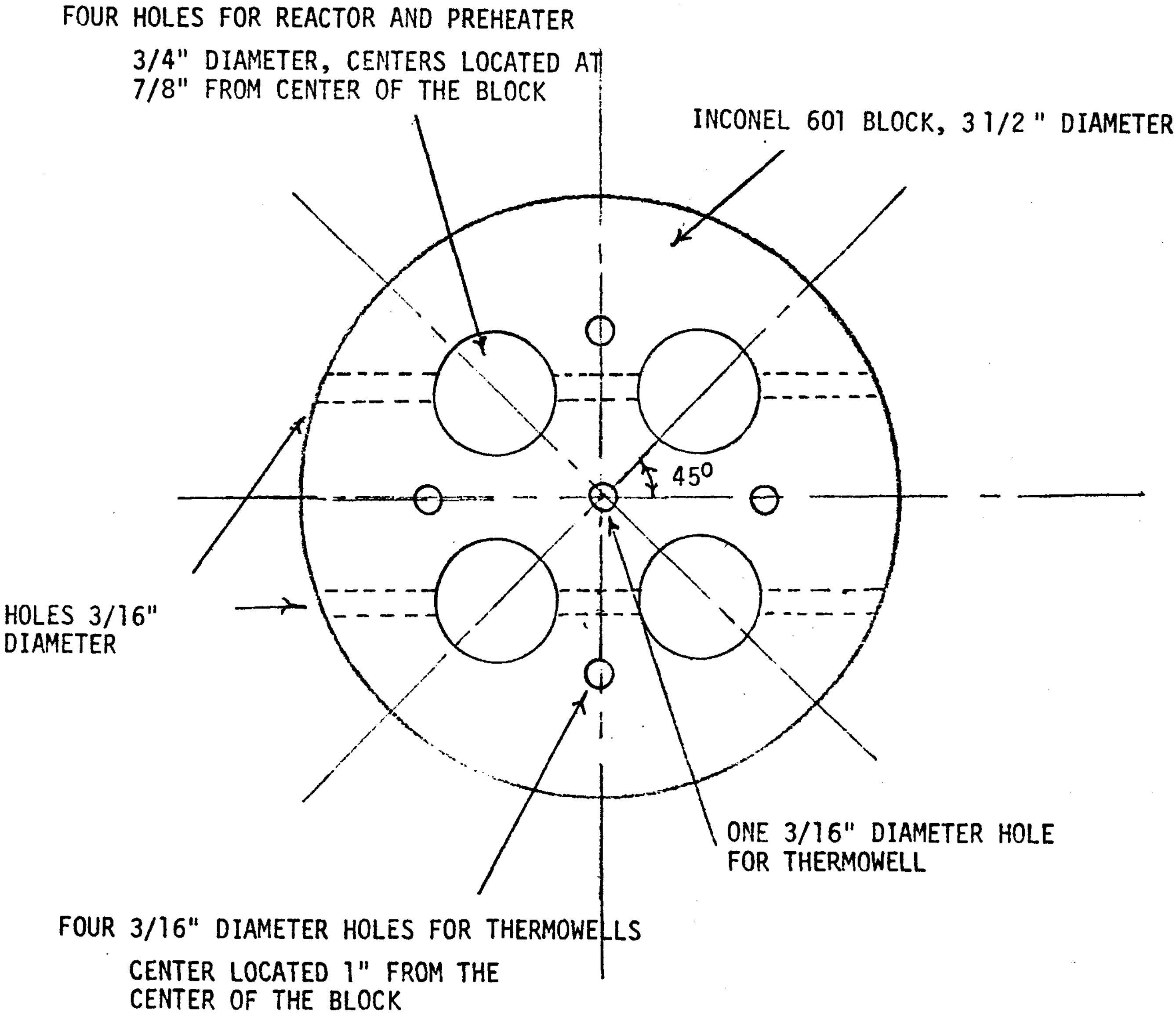

FIGURE 12

SCHEMATIC FLOW DIAGRAM OF THE PILOT UNIT

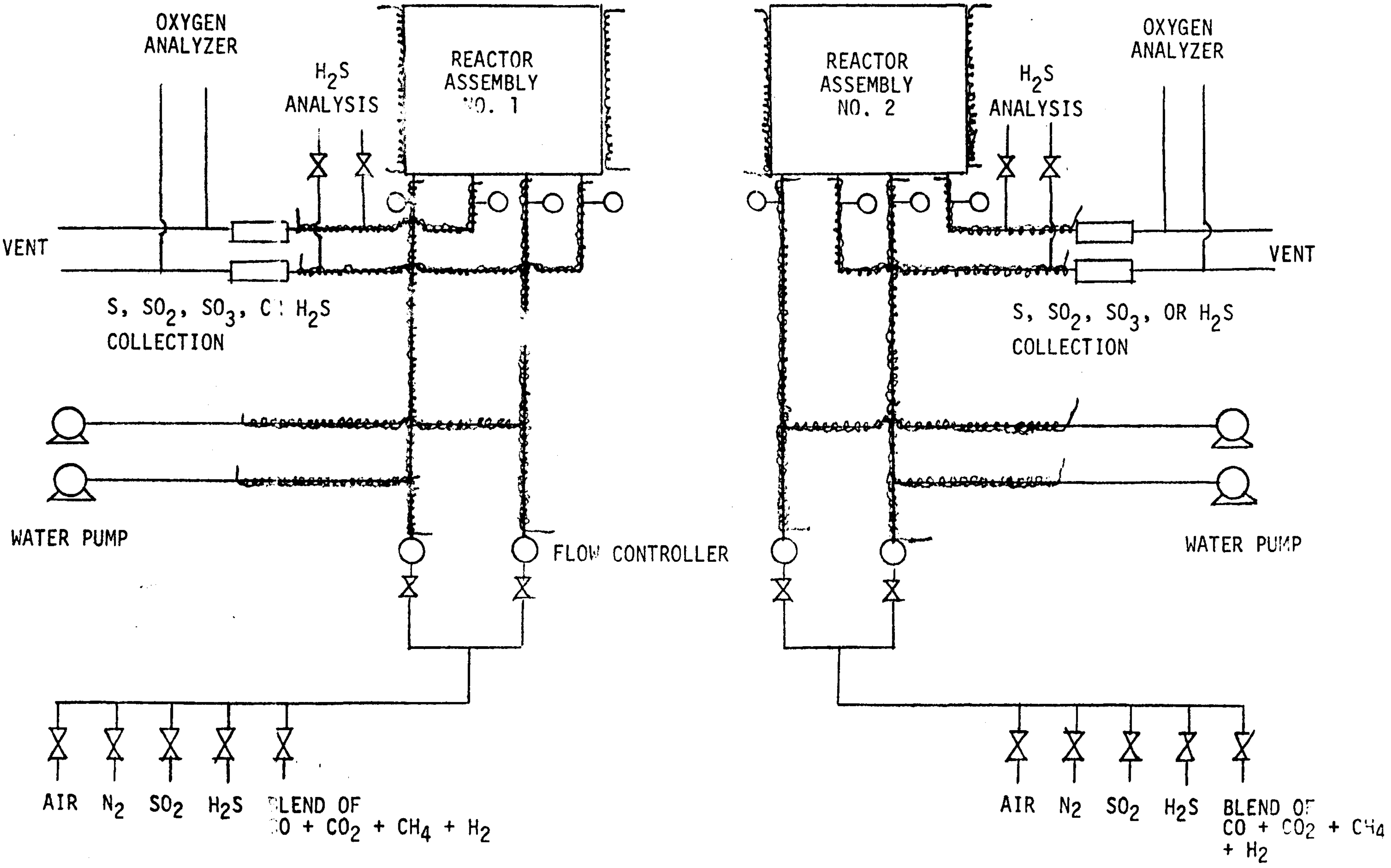

D. Simulation of Temperature Exotherms and Breakthrough Curves

During the work done under ERDA Contract E(49-18)2033 for iron oxide desulfurization of hot low Btu producer gas, several mathematical models describing the absorption and regeneration process were developed. Experimentally obtained data were correlated using two levels of model confirmation criteria:

(1) Level 1 Confirmation

The model must be able to predict the shapes of the experimentally observed breakthrough curves during absorption and regeneration.

(2) Level 2 Confirmation

The model must be able to predict the experimentally observed effects of design variables on the absorption efficiency and regeneration efficiency.

The final report for ERDA Contract E(49-18)2033 discusses this in-depth. A semi-empirical model was found to satisfy both criteria well for absorption. The regeneration data were best explained by a kinetic model.

Task I of the new ERDA Contract 87-7-1513 consists of applying APCI-developed mathematical model to data obtained by MERC.

During this month several computer simulation runs were made. Objectives of this exercise were:

(1) To determine the validity of APCI model, using the most rigorous criteria of simulating the entire temperature exotherms and breakthrough curves.

(2) To decide on the information required of MERC to complete Task I.

Two absorption runs and two regeneration runs were simulated. These runs are representative of typical runs. The runs were made at several values of heat balance number and gas adiabatic temperature rise. Results of these simulations will be discussed in detail in the next monthly report. Preliminary conclusions are:

(1) The model can predict shapes of breakthrough curves and effects of design variables on efficiencies very well for both absorption and regeneration.

(2) The model can predict entire hydrogen sulfide breakthrough curves for absorption very well.

(3) The model can predict oxygen breakthrough curves for regeneration quite well up to 50% oxygen breakthrough.

(4) The model does not predict the temperature exotherms observed in regeneration. However, since it overpredicts the temperatures, it could be used as a conservative criteria for design. Possible reasons for this discrepancy are non-adiabaticity of operation, simultaneous elemental sulfur formation, and axial dispersion.

E. Preparation of Guidelines for Economic Evaluation

A preliminary economic evaluation and cost-sensitivity analysis of some process variables will be done as Task 3 of this contract. The specific items to be considered and ranges of variables are proposed. These guidelines are being finalized after discussions with our Process Engineering Group. An outline of the approach to economic evaluation will be given in the next monthly report.

II. FUTURE WORK

Plans for next month include:

(1) Visit Morgantown Energy Research Center to obtain data for Task I.

(2) Finalize guidelines for Task 3 and start economic evaluations.

(3) Apply APCI model to MERC data.

(4) Procure reactor blocks and machine them to build reactors.